

Signatures of Chiral Magnetic Effect in the Collisions of Isobars

Shuzhe Shi,² Hui Zhang,^{3,1} Defu Hou,^{1,*} and Jinfeng Liao^{4,†}

¹*Institute of Particle Physics (IOPP) and Key Laboratory of Quark and Lepton Physics (MOE), Central China Normal University, Wuhan 430079, China.*

²*Department of Physics, McGill University, 3600 University Street, Montreal, QC, H3A 2T8, Canada.*

³*Institute of Quantum Matter, South China Normal University, Guangzhou 510006, China.*

⁴*Physics Department and Center for Exploration of Energy and Matter, Indiana University, 2401 N Milo B. Sampson Lane, Bloomington, IN 47408, USA.*

(Dated: March 28, 2022)

Quantum anomaly is a fundamental feature of chiral fermions. In chiral materials the microscopic anomaly leads to nontrivial macroscopic transport processes such as the Chiral Magnetic Effect (CME), which has been in the spotlight lately across several branches of physics. The quark-gluon plasma (QGP) created in relativistic nuclear collisions provides the unique example of a chiral material consisting of intrinsically relativistic chiral fermions. Potential discovery of CME in QGP is of utmost significance and extensive experimental searches have been carried out over the past decade. A decisive new collider experiment, dedicated for possibly detecting CME in the collisions of isobars, has been performed in 2018 with analysis underway. In this paper, we develop the necessary and state-of-the-art theoretical tool for describing CME phenomenon in these collisions and propose an appropriate isobar subtraction strategy for the best background removal. Based on that, we make quantitative predictions for signatures of CME in the collisions of isobars.

I. INTRODUCTION

The investigation of novel quantum transport in chiral materials is a rapidly growing area of research that has attracted significant interests and activities recently from a broad range of physics disciplines such as high energy physics and condensed matter physics. Chiral materials are many-body quantum systems that consist of massless fermions (i.e. chiral fermions) that are either fundamental particles or emergent quasi-particles behaving as chiral fermions. A notable example of the former, is the so-called quark-gluon plasma (QGP) which is a new phase of hadronic matter existing at primordially high temperatures available in the early Universe and which is now recreated in laboratories by high energy nuclear collisions. The novel examples of the latter, include the latest discovered topological phases of condensed matter systems known as Dirac and Weyl semimetals. For recent reviews, see e.g. [1–10].

The most salient feature of chiral fermions is the chiral anomaly under the presence of gauge interactions. Chiral materials manifest such *microscopic quantum peculiarity* through unique *macroscopic anomalous transport properties* in highly nontrivial ways. Quantum transport processes that are forbidden in normal environment become possible (and necessary) in such chiral materials. A famous example among this type of anomalous chiral transport is the so-called Chiral Magnetic Effect (CME), predicting the generation of an electric current in chiral materials as response to an applied magnetic field. The CME is a remarkable example as a new kind of quantum electricity that one may tentatively call “magne-tricity”.

The observation of CME in various physical systems is of fundamental importance. In semimetal systems the CME-induced transport has been measured via observables like negative magnetoresistance [11–14]. In the subatomic chiral material, i.e. the quark-gluon plasma created in relativistic nuclear collisions, enthusiastic efforts have been made to look for evidences of CME at the Relativistic Heavy Ion Collider (RHIC) and the Large Hadron Collider (LHC) [15–25]. While lots of measurements have been accumulated so far from RHIC and LHC with encouraging hints, the interpretation of these data remains inconclusive due to significant background contamination — see detailed discussions in e.g. [26, 27].

An unambiguous observation of CME in the subatomic system would not only be the first confirmation of this novel effect in a chiral material of intrinsic relativistic fermions, but also provide tantalizing experimental verification for the high-temperature restoration of a spontaneously broken global symmetry (the chiral symmetry) which is a fundamental prediction of the basic theory for strong nuclear force known as Quantum Chromodynamics (QCD). It would additionally open a unique window for characterizing the intriguing topological fluctuations of gluon fields — the non-Abelian gauge fields of QCD. Given such importance, a decisive isobaric collision experiment has been carried out in the 2018 RHIC Run, with the dedicated physics goal of discovering the CME [28, 29]. The basic idea is to contrast the CME-sensitive observables in two different colliding systems, the RuRu and the ZrZr, where the Ru and Zr are a pair of isobars with the same nucleon numbers ($A = 96$) but different nuclear charges ($Z = 44$ and $Z = 40$ respectively). The expectation is that the two systems will have the *same* background contributions while quite *different* CME signals due to the difference in their nuclear charge and thus magnetic field strength. This experiment offers

* houdf@mail.ccnu.edu.cn

† liaoji@indiana.edu

the unique opportunity to detect CME in such collisions and currently the data analysis is actively underway.

The present work focuses on quantitative predictions for the signatures of CME in the isobaric collision experiments. For that purpose, we develop a state-of-the-art tool and the first of its kind, the EBE-AVFD (event-by-event anomalous-viscous fluid dynamics), that can characterize CME signals from dynamical anomalous transport as well as account for background correlations in a realistic heavy ion collision environment. With this powerful tool, we compute CME observables and present results that shall soon be tested by experimental measurements. The rest of this paper is organized as follows. A detailed discussion of methodology will be given in Section II. The main results, namely predictions for a number of CME observables in isobaric collisions, will be presented in Section III. We conclude in Section IV.

II. METHODOLOGY

In the context of heavy ion collisions, the Chiral Magnetic Effect induces an electric current along the magnetic field arising mainly from the fast-moving spectator protons. The azimuthal orientation of this field is approximately perpendicular to the reaction plane (RP) [30], and therefore the CME current will lead to a charge separation across the reaction plane. Such a charge separation can be measured by the charge asymmetry in azimuthal correlations of same-sign (SS) and opposite-sign (OS) charged hadron pairs. There are however charge-dependent correlations from backgrounds other than the CME that would contribute substantially to the relevant observables, with resonance decays and local charge conservation (LCC) being dominant sources. To unambiguously extract a clean CME signal from the background-contaminated measurements has proven extremely challenging. To resolve such pressing issue and pave the way for potential discovery of CME would require: (1) a sophisticated and realistic simulation framework that can quantitatively characterize backgrounds and predict the signatures of CME; (2) an experimental analysis approach to subtract out backgrounds in a model-independent way. In the following, we discuss our methodology that would address these requirements.

A. The EBE-AVFD Framework

In relativistic heavy ion collisions, the dynamical evolution of the produced bulk matter has a dominant hydrodynamic stage that is well modeled by relativistic viscous fluid dynamics [31, 32]. In order to quantitatively describe CME-induced signatures in these collisions, one needs to account for the anomalous charge transport current in the dynamically evolving bulk fluid. Conventional fluid dynamics does not include such macroscopic chiral effect and a new framework is needed. The theo-

retical foundation of anomalous fluid dynamics has been laid down in [33]. Based on that, a fluid dynamical realization of CME transport in modeling heavy ion collisions has been achieved through the development of the Anomalous-Viscous Fluid Dynamics (AVFD) framework [34, 35]. The AVFD provides the unique and versatile simulation tool for quantitative computation of CME-induced charge separation. Important features of CME signals have been characterized with AVFD simulations [34]. (We note in passing that there have also been efforts in simulating CME signals based on non-hydrodynamic models [36–38].)

The AVFD framework can be briefly summarized as follows [34]. It describes the charge transport by solving the fluid dynamical evolution of the fermion currents (i.e. the quark currents of various flavors and chirality) in the system perturbatively on top of the neutral bulk fluid evolution as specified by the space-time dependent temperature field $T(x^\mu)$ and fluid velocity field $u^\nu(x^\mu)$. The corresponding fluid dynamical equations, including both usual viscous transport and new anomalous transport for these fermion currents, take the following form:

$$\hat{D}_\mu J_{\chi,f}^\mu = \chi \frac{N_c Q_f^2}{4\pi^2} E_\mu B^\mu \quad (1)$$

$$J_{\chi,f}^\mu = n_{\chi,f} u^\mu + \nu_{\chi,f}^\mu + a_{\chi,f}^\mu \quad (2)$$

$$a_{\chi,f}^\mu = \chi \frac{N_c Q_f}{4\pi^2} \mu_{\chi,f} B^\mu \quad (3)$$

$$\Delta_\nu^\mu \hat{d}(\nu_{\chi,f}^\nu) = -\frac{1}{\tau_r} \left[\left(\nu_{\chi,f}^\mu \right) - \left(\nu_{\chi,f}^\mu \right)_{NS} \right] \quad (4)$$

$$\left(\nu_{\chi,f}^\mu \right)_{NS} = \frac{\sigma}{2} T \Delta^{\mu\nu} \partial_\nu \left(\frac{\mu_{\chi,f}}{T} \right) + \frac{\sigma}{2} Q_f E^\mu \quad (5)$$

where $\chi = \pm 1$ labels chirality for RH/LH currents and f labels different quark flavors with their respective electric charge Q_f and with color factor $N_c = 3$. It should be particularly emphasized that the new term $a_{\chi,f}^\mu$ defined in Eq.(3) implements explicitly the CME current. Its sign changes with the chirality χ , which reflects the feature of anomalous transport where the direction of the CME current is opposite for RH and LH particles. The $E^\mu = F^{\mu\nu} u_\nu$ and $B^\mu = \frac{1}{2} \epsilon^{\mu\nu\alpha\beta} u_\nu F_{\alpha\beta}$ represent the external electromagnetic fields in fluid's local rest frame. In the above the projection operator is $\Delta^{\mu\nu} = (g^{\mu\nu} - u^\mu u^\nu)$ where u^μ is the fluid velocity field, and the differential operator is $\hat{d} = u^\mu \hat{D}_\mu$ with \hat{D}_μ as the covariant derivatives in the coordinates (τ, x, y, η) commonly used for heavy ion collisions. The fermion densities $n_{\chi,f}$ and corresponding chemical potential $\mu_{\chi,f}$ are related by lattice-computed quark number susceptibilities $c_2^f(T)$ [39]. It is also worth emphasizing that the above framework includes the normal viscous transport currents $\nu_{\chi,f}^\mu$ at the second-order of gradient expansion, which is important for providing a realistic and quantitative description of charge transport in consistency with the background bulk flow which is also described by the 2nd-order viscous hydrodynamics. Two transport coefficients (characterizing normal viscous effects) are the nor-

mal diffusion coefficient σ and relaxation time τ_r . The bulk fluid fields $T(x^\mu)$ and $u^\nu(x^\mu)$ are determined from widely-adopted and data-validated hydrodynamic simulations like VISHNU [31] and MUSIC [32].

However, a few crucial elements were missing in the aforementioned AVFD framework. First, the background correlations that make dominant contributions to the measured observables are not implemented. Second, event-by-event fluctuations are known to play very important roles in various heavy ion collision observables and must be accounted for in order to make realistic and quantitative predictions. Third, for collision energies at RHIC, a hadron cascade stage following the fluid dynamics evolution is also known to be necessary for accurately computing various observables. These missing key elements prevent one from making reliable predictions for the important isobaric collision experiments.

In the present work, we've successfully addressed these outstanding challenges by developing a new powerful tool called Event-By-Event Anomalous-Viscous Fluid Dynamics (EBE-AVFD). In the EBE-AVFD, the initial state fluctuations are fully accounted for by event-wise sampling for bulk entropy density and the fermion axial charge density. Following the end of hydrodynamic stage for each bulk event evolution, hadrons are sampled by maintaining charge conservations and then further evolved through hadron cascade stage via URQMD simulations. This framework for the first time allows a quantitative and consistent evaluation of both CME signals and background correlations within the same realistic bulk evolution. The EBE-AVFD represents the state-of-the-art tool for reliable predictions of various CME-related measurements in heavy ion collisions.

We end with a brief remark on the magnetic field in these collisions, which plays a central role for inducing the CME signal in QGP. The initial vacuum magnetic field, mainly from spectators reaching peak values on the order of pion-mass-square (or $\sim 10^{13}$ Tesla, has been well modeled on event-by-event basis in great details (see e.g. [30]). Its subsequent time duration is however uncertain at the moment, with lots of efforts to constrain it via theoretical calculations and phenomenological extractions [30, 40–49]. In this work, we adopt a phenomenologically tested parameterization $B(\tau) = B_0/[1 + (\tau/\tau_0)^2]$ (where B_0 the peak value from initial state simulations) with a reasonable lifetime parameter $\tau_0 = 0.6$ fm/c [47, 48].

B. Comparison Strategy for Isobaric Collisions

The key for success of the isobaric contrast idea, is to make sure that *one has two collections of collision events from RuRu and ZrZr systems respectively that must be identical in their bulk properties (in particular the multiplicity and elliptic flow v_2)*. In conventional analysis one would select events based on centrality (i.e. multiplicity) and then compare RuRu with ZrZr systems at same centrality. The underlying assumption would be that they

would have identical bulk flow and background correlations. It turns out that such assumption may not be entirely true. Recent simulations of initial geometry in these collisions suggest potential difference at a few percent level in their elliptic eccentricity (even within the same centrality class) due to uncertainty in the nucleon distributions in the isobar pair of nuclei [50, 51]. This presents enough of concern which may complicate the supposedly “clean” comparison between the isobars at quantitative level, especially given the rather small CME signal. To address this important issue and to ensure a successful isobar contrast, we propose a new strategy for comparing the isobaric systems, namely to use a joint (multiplicity + elliptic flow) event selection method [51]. We demonstrate the effectiveness of this strategy with event-by-event simulations of initial conditions.

In Fig. 1 we first examine the usual centrality class event selection by showing the comparison between the initial conditions of RuRu versus ZrZr collisions based on that method: left panel for relative difference in eccentricity $\Delta\langle\epsilon_2\rangle \equiv \langle\epsilon_2\rangle^{Ru} - \langle\epsilon_2\rangle^{Zr}$ while right panel for relative difference in the (event-wise out-of-plane-projected) magnetic-field-strength-squared $\Delta(B_{sq}) \equiv \langle B_{out}^2\rangle^{Ru} - \langle B_{out}^2\rangle^{Zr}$. The simulations are performed with Monte-Carlo Glauber model, for three different Woods-Saxon (WS) nucleon distributions: WS for the spherical case, WS1 for the case of more quadrupole deformation in Ru nucleus while WS2 for the case of more quadrupole deformation in Zr nucleus [28]. As one can see from Fig. 1, within a given centrality class and depending on specific nucleon distributions, the two systems could still have a few percent level of difference in their elliptic eccentricity (especially toward central and semi-central collisions) which is directly related to the expected difference in their background correlations. Their relative difference in magnetic field strength, which drives the signal, is at the level of 10 ~ 25%. The “separation” between $\Delta\langle\epsilon_2\rangle$ and $\Delta(B_{sq})$ is about one order of magnitude, which may or may not be enough. This critically depends on the signal-to-background ratio in the correlation observables. If the signal fraction would be very small, then contrasting the isobar pairs may not work well with the conventional centrality selection.

We now examine the proposed *joint (multiplicity + elliptic-flow) event selection* method for selecting and comparing two truly identical collections of isobar events. This can be done by the following procedure applied identically to RuRu and ZrZr collisions: (a) first binning all events according to multiplicity (or equivalently centrality), (b) then applying a further geometric cut on eccentricity ϵ_2 (or equivalently on final state elliptic flow v_2) cut for the events within a given centrality. Note practically the ϵ cut range should be chosen to be around the mean values of that centrality with a span that is not too narrow to ensure enough statistics while not too wide, so as to select the “most typical” events for a given centrality and to drop out the “weird events” from unusual fluctuations. The important point is to apply *the same*

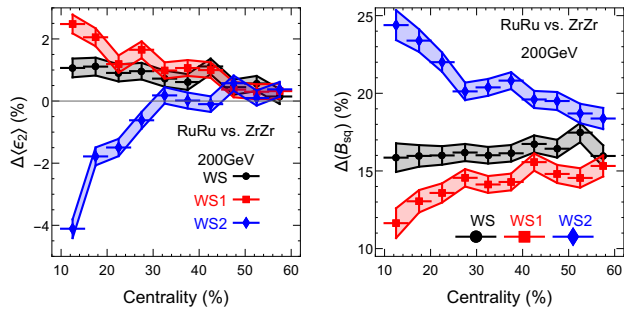


FIG. 1. (Color online) The relative difference in eccentricity $\Delta\langle\epsilon_2\rangle$ (left) and projected magnetic-field-strength-squared $\Delta(B_{sq})$ (right) between RuRu and ZrZr, with conventional centrality event selection.

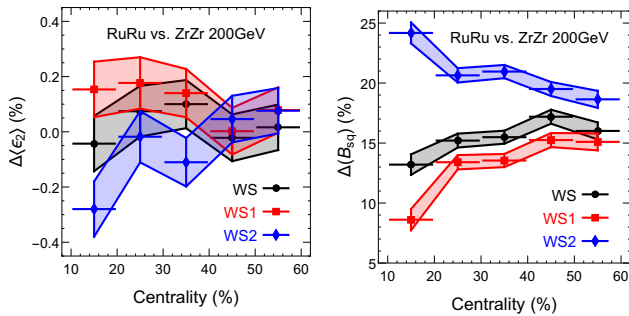


FIG. 2. (Color online) The relative difference in eccentricity $\Delta\langle\epsilon_2\rangle$ (left) and projected magnetic-field-strength-squared $\Delta(B_{sq})$ (right) between RuRu and ZrZr, with the proposed joint (multiplicity + elliptic-flow) event selection.

multiplicity and geometry selection for both RuRu and ZrZr events. As a test of this idea, we use the same set of initial condition samples as that of Fig. 1 above and apply the proposed cut on the initial entropy (as proxy for multiplicity) and eccentricity (as proxy for v_2). With the so-selected event samples, we compare again the relative difference between RuRu and ZrZr systems: see Fig. 2. As one can see: the relative difference in geometry $\Delta\langle\epsilon_2\rangle$ is now reduced to the level of $\sim 0.1\%$ between the two isobars while that in magnetic field $\Delta(B_{sq})$ remains at the 10 \sim 25% level. The “separation” between the two has now become about two orders of magnitude for all centrality and the contrast between RuRu and ZrZr are most likely able to reveal potential magnetic-field-driven CME signal despite our imperfect knowledge about the initial nucleon distributions.

We have extensively verified the effectiveness of this proposed comparison strategy based on joint (multiplicity + elliptic flow) event selection for a variety of different nucleon distributions beyond just the Woods-Saxon types. This strategy has also been validated directly with the final state events generated from our AVFD simulations. In the following, we will adopt this strategy and make predictions for various observables.

III. PREDICTIONS FOR ISOBARIC COLLISIONS

In this section, we present the EBE-AVFD predictions for isobaric collisions based on the aforementioned comparison strategy. Here we focus on collision events corresponding to the usual 40 \sim 50% centrality range and have generated ten millions of collision events for each of the RuRu and ZrZr systems. For each system, EBE-AVFD simulations are done for 10^5 different hydrodynamic initial profiles, with 100 hadron cascade events following each hydrodynamic profile. We apply the identical joint cut for charged particle multiplicity N_{ch} and elliptic flow v_2 : $65 \leq N_{ch}^{ch}|_{|y|<1} \leq 96$ and $0.05 < v_2 < 0.25$ for both systems. The v_2 is measured for charged particles in the kinematic region $0.15 < p_T < 2\text{GeV}$ and $|y| < 1$ with event-plane (EP) determined from reference particles in the rapidity range $1.5 < |y| < 4.0$. This procedure selects about 44% of all the simulation events we generated. As a consistency check, we have compared the measured charged particle multiplicity and v_2 distributions of the post-selection events: both RuRu and ZrZr events are found to be identical, with the same average $\langle N_{ch} \rangle = 80.4$ and standard deviation 8.5 as well as with the same $\langle v_2 \rangle = 0.1132$ and standard deviation 0.046. This procedure thus guarantees the same background contributions for the isobar pairs. We also note that the v_2 cut has the added benefit of improving event-plane resolutions.

With the selected events we then perform physical analysis of various CME-motivated correlation observables. Specifically we propose to examine the absolute difference between RuRu and ZrZr systems in these observables. Such a procedure of taking the absolute difference would simply subtract out the background portion (which is guaranteed to be identical between the isobars by the proposed event-selection). What potentially remains from such subtraction would be the pure CME signal (or more precisely the difference in the CME signal between RuRu and ZrZr systems).

Before proceeding to show concrete results, we point out a few characteristic features that would be expected for a pure CME signal (obtained only after removal of backgrounds from usual contaminated correlations via isobar subtraction). The strength of such a signal as revealed in charge-dependent correlators shall be quadratically dependent on the amount of initial axial charge. The correlations from such a signal shall be along the magnetic field direction which is on average along the out-of-plane direction but azimuthally fluctuates around it [30]. Specifically the signal’s orientation would have different degrees of correlation with the so-called event-plane (EP) geometry and the reaction-plane (RP) geometry. These features would provide very useful validation of the EBE-AVFD predictions for isobaric collisions, as we shall demonstrate below.

A. Charge-Dependent Azimuthal Correlations

The charge transport due to CME current will lead to a *charge separation* along the magnetic field direction in the fireball created in heavy ion collisions. It is this charge separation effect that one tries to measure with various azimuthal correlation observables. The frequently used γ -correlator is defined as [52]:

$$\gamma^{\alpha\beta} = \langle \cos(\phi^\alpha + \phi^\beta - 2\Psi_2) \rangle \quad (6)$$

where Ψ_2 should ideally be the reaction plane (RP) but is practically identified via the 2nd harmonic event plane (EP) as an experimental proxy. The correlation of pairs with same electric charge, γ^{SS} , has $\{\alpha\beta\} \rightarrow \{++\}$ or $\{--\}$ while that for opposite charged pairs, γ^{OS} , has $\{\alpha\beta\} \rightarrow \{+-\}$ or $\{-+\}$. To maximize the signal and reduce the backgrounds, one can further examine the difference between the correlation of same and opposite charged pairs, $\gamma^{OS-SS} = \gamma^{OS} - \gamma^{SS}$, in which the charge-independent backgrounds cancel out. Another closely related and very useful observable is the δ -correlator [26, 53]

$$\delta^{\alpha\beta} = \langle \cos(\phi^\alpha - \phi^\beta) \rangle. \quad (7)$$

Similarly one can examine $\delta^{OS-SS} = \delta^{OS} - \delta^{SS}$.

A pure CME-induced charge separation dipole would contribute to the above correlators as : $\gamma_{CME}^{OS-SS} \rightarrow 2\langle a_1^2 \cos(2\Psi_B - 2\Psi_2) \rangle$ and $\delta_{CME}^{OS-SS} \rightarrow -2\langle a_1^2 \rangle$ where a_1 is the event-wise charge separation dipole from CME transport along the magnetic field direction Ψ_B and the factor $\cos(2\Psi_B - 2\Psi_2)$ captions the azimuthal decorrelation between Ψ_B and bulk geometry orientation Ψ_2 . However, CME contributions could not be easily extracted from current measurements of γ and δ correlators due to dominant non-CME background contributions [53–61]. This is where the isobar contrast would be uniquely valuable in providing a direct access to pure CME signals after background subtraction procedure discussed in the previous section. Specifically, we will focus on their difference: $\gamma_{Ru-Zr}^{OS-SS} = \gamma_{RuRu}^{OS-SS} - \gamma_{ZrZr}^{OS-SS}$ and $\delta_{Ru-Zr}^{OS-SS} = \delta_{RuRu}^{OS-SS} - \delta_{ZrZr}^{OS-SS}$. We emphasize that once backgrounds are removed, both γ and δ correlators are sensitive to the presence of CME contributions.

In Fig. 3 (upper panel) we show predictions from EBE-AVFD simulations for observables γ_{Ru-Zr}^{OS-SS} and δ_{Ru-Zr}^{OS-SS} with respect to event-plane (EP) geometry (i.e. $\Psi_2 \rightarrow \Psi_{EP}$), for four different levels of initial axial charge density n_5 (normalized by the initial entropy density s of bulk hydrodynamics) at $n_5/s = 0\%, 5\%, 10\%$ and 20% respectively. The error bars are statistical uncertainty from simulations which are mainly limited by number of AVFD events and thus by available computation time. We note that the expected isobar analysis statistical uncertainty could be smaller than our simulations by nearly an order of magnitude based on the collected isobar events and therefore would have significant capability to differentiate a nonzero signal from a null result. While the level

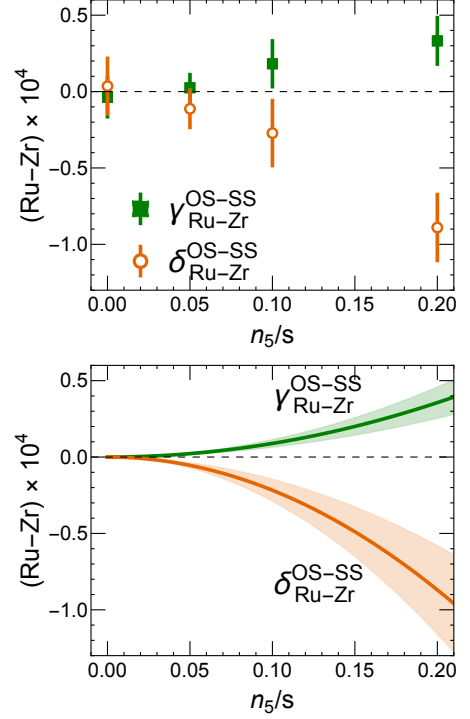


FIG. 3. (color online) Predictions from EBE-AVFD simulations for observables γ_{Ru-Zr}^{OS-SS} and δ_{Ru-Zr}^{OS-SS} with respect to event-plane (EP) geometry (i.e. $\Psi_2 \rightarrow \Psi_{EP}$) for $n_5/s = 0\%, 5\%, 10\%$ and 20% respectively in the upper panel, along with quadratic fitting results in the lower panel. The error bars in upper panel are statistical uncertainty and the shaded bands in lower panel indicate fitting uncertainty.

of initial axial charge presents the major source of theoretical uncertainty, the quantitative consistency between γ and δ correlators would provide sufficient validation of CME-signal and help constrain the initial axial charge.

The CME-induced correlations are expected to depend quadratically upon the initial axial charge density n_5 . The simulation results indeed clearly show such a trend. In Fig. 3 (lower panel) we present a quadratic fitting to the simulation results, which are also summarized below:

$$\gamma_{Ru-Zr}^{OS-SS} \Big|_{EP} \simeq (0.89 \pm 0.51) \times 10^{-3} \times \left(\frac{n_5}{s}\right)^2 \quad (8)$$

$$\delta_{Ru-Zr}^{OS-SS} \Big|_{EP} \simeq -(2.17 \pm 0.72) \times 10^{-3} \times \left(\frac{n_5}{s}\right)^2 \quad (9)$$

The above results have further motivated us to propose a new observable ζ_{isobar} built from the ratio between the two correlators after isobar subtraction:

$$\zeta_{isobar}^{EP} \equiv \frac{\gamma_{Ru-Zr}^{OS-SS} \Big|_{EP}}{\delta_{Ru-Zr}^{OS-SS} \Big|_{EP}} \simeq -(0.41 \pm 0.27) \quad (10)$$

The advantage of this ratio is that it is *independent* of the (uncertain) initial axial charge and therefore could

provide a robust test of CME. We note this ratio essentially “picks up” the azimuthal de-correlation factor $\cos(2\Psi_B - 2\Psi_{EP})$, which is also computed from our simulation events to have an average value about 0.46 and found to be quantitatively consistent with the magnitude of the above ratio. We emphasize again, that these features are specific to pure CME signal and are manifested only by virtue of isobar subtraction that would remove all backgrounds.

B. Reaction Plane versus Event Plane

It was proposed recently that comparing correlators measured with respect to reaction plane (RP) and to event plane (EP) could provide a useful way to help decipher CME signal [58]. The point is that the magnetic field and thus the CME-induced charge dipole have different degrees of azimuthal de-correlations with RP and with EP. The difficulty with the RP measurements is that in principle the RP is a theoretical concept and one has to use certain experimental proxy for it like the spectator plane (to be inferred from e.g. ZDC component of STAR detector). Nevertheless it would be interesting to examine correlators with respect to RP.

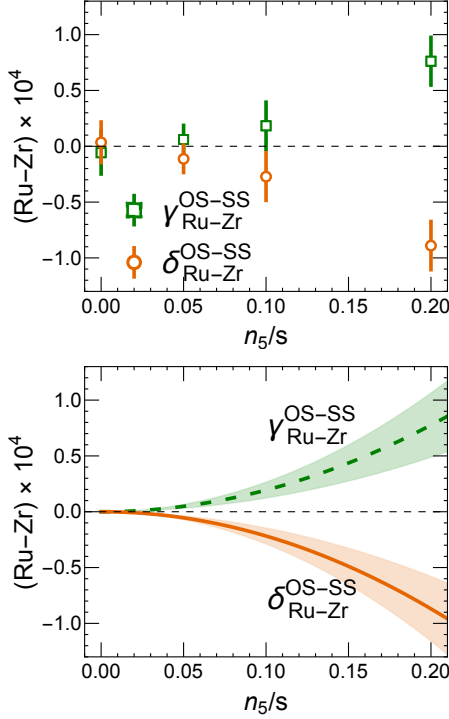


FIG. 4. (color online) Predictions from EBE-AVFD simulations for observables γ_{Ru-Zr}^{OS-SS} and δ_{Ru-Zr}^{OS-SS} with respect to reaction-plane (RP) geometry (i.e. $\Psi_2 \rightarrow \Psi_{RP}$) for $n_5/s = 0\%, 5\%, 10\%$ and 20% respectively in the upper panel, along with quadratic fitting results in the lower panel. The error bars in upper panel are statistical uncertainty and the shaded bands in lower panel indicate fitting uncertainty.

In Fig. 4 (upper panel) we show predictions from EBE-AVFD simulations for observables γ_{Ru-Zr}^{OS-SS} and δ_{Ru-Zr}^{OS-SS} with respect to reaction-plane (RP) geometry (i.e. $\Psi_2 \rightarrow \Psi_{RP}$), for four different levels of initial axial charge density n_5 (normalized by the initial entropy density s of bulk hydrodynamics) at $n_5/s = 0\%, 5\%, 10\%$ and 20% respectively. Compared with the EP results in Fig. 3, the γ correlator becomes larger due to a stronger correlation between magnetic field direction and the RP, and the δ correlator is identical between the RP and the EP as one would expect.

In Fig. 3 (lower panel) we present a quadratic fitting to the simulation results for the RP measurements, which are also summarized below:

$$\gamma_{Ru-Zr}^{OS-SS} \Big|_{RP} \simeq (1.94 \pm 0.72) \times 10^{-3} \times \left(\frac{n_5}{s}\right)^2 \quad (11)$$

$$\delta_{Ru-Zr}^{OS-SS} \Big|_{RP} \simeq -(2.17 \pm 0.72) \times 10^{-3} \times \left(\frac{n_5}{s}\right)^2 \quad (12)$$

The RP result for the ratio observable ζ_{isobar} is:

$$\zeta_{isobar}^{RP} \equiv \frac{\gamma_{Ru-Zr}^{OS-SS} \Big|_{RP}}{\delta_{Ru-Zr}^{OS-SS} \Big|_{RP}} \simeq -(0.90 \pm 0.45) \quad (13)$$

The magnitude of the ratio from RP is about twice that from EP. This is again quantitatively consistent with the azimuthal de-correlation factor in the RP case, i.e. $\cos(2\Psi_B - 2\Psi_{RP})$ which has an average value about 0.95. A series measurements of these correlators and the proposed ratios with respect to both EP and RP would provide a set of stringent tests for validating and constraining the exist of CME signals in isobaric collisions.

C. Event-Shape Dependence

One way of revealing the background contributions in the “raw” correlators (e.g. un-subtracted γ -correlator) is to examine how the correlators change with the event-wise geometry of the bulk matter [19]. This can be experimentally done by the so-called event-shape-engineering method. By grouping events in a given centrality into different bins based on elliptic flow cuts and measuring the correlators in each bin, one indeed observes a clear dependence of γ -correlator on bulk v_2 which is not a feature of CME but a feature of several identified background sources. The event-shape analysis provides a possible way of separating backgrounds from CME signal.

A pure CME signal, on the other hand, should be (nearly) independent of event shape. This can provide an additional important consistency check on the CME signal to be derived from isobar subtraction. In Fig. 5 we show EBE-AVFD results for the dependence of observables γ_{Ru-Zr}^{OS-SS} and δ_{Ru-Zr}^{OS-SS} on event shape. In this analysis, we use three identical bins for RuRu and ZrZr systems: $v_2 \in (0.01, 0.055)$, $v_2 \in (0.055, 0.11)$ and

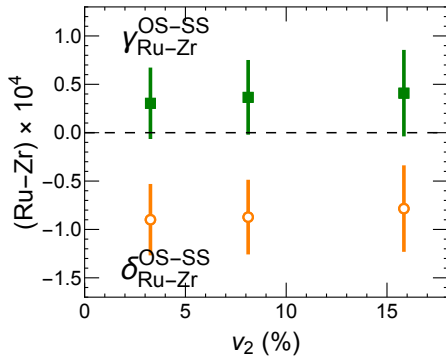


FIG. 5. (color online) Predictions from EBE-AVFD simulations for observables γ_{Ru-Zr}^{OS-SS} and δ_{Ru-Zr}^{OS-SS} as a function of bin-wise elliptic flow v_2 from event-shape analysis with three identical bins for RuRu and ZrZr systems. The simulation results are obtained with $n_5/s = 20\%$.

$v_2 \in (0.11, 0.30)$. We've checked that the average multiplicity and elliptic flow in each bin are identical between the isobars. The correlators are then measured in each bin and subtracted between isobars to produce the results in Fig. 5. We indeed observe that both γ and δ correlators are nearly independent of the event shape. One could quantify this dependence via a linear fitting for $\frac{\gamma}{\gamma_{mid-bin}}$ versus $\frac{v_2}{v_{2mid-bin}}$ (and similarly for the δ). The extracted slopes are (0.18 ± 0.98) for γ and (-0.08 ± 0.41) for δ , both consistent with being zero.

D. The R-Correlator

Finally we present the EBE-AVFD results for a different category of correlator, the R-correlator proposed in [62, 63]. This correlator is built via multiple steps. For a given event, one first examines the distribution $C^{\parallel}(\Delta S)$ for a charge dipole ΔS along out-of-plane direction (with respect to EP) normalized by the same distribution obtained from the same event after random shuffling of charges. One then examines a similar distribution $C^{\perp}(\Delta S)$ along the in-plane direction. In the last step one takes a ratio between the two: $R(\Delta S) = C^{\parallel}(\Delta S)/C^{\perp}(\Delta S)$. This correlator has been demonstrated with quantitative simulations to have certain advantages in suppressing the background correlations. Whether all background correlations would be completely removable in such a correlator, remains unclear at the moment.

To make predictions for isobaric collisions, we again examine the isobar-subtracted correlator: $[R_{Ru}(\Delta S) - R_{Zr}(\Delta S)]$ which shall be background free. In Fig. 6 we show the EBE-AVFD results for the R-correlator distributions for $n_5/s = 0\%, 5\%, 10\%$ and 20% respectively. As one can see, the R-correlator (after isobar subtraction) is basically flat for the none-CME case ($n_5/s = 0\%$) while becomes more and more upward concave with in-

creasingly strong CME signal. A precise measurement of the R-correlator with enough statistics should provide a further independent and important validation for the presence of CME signal.

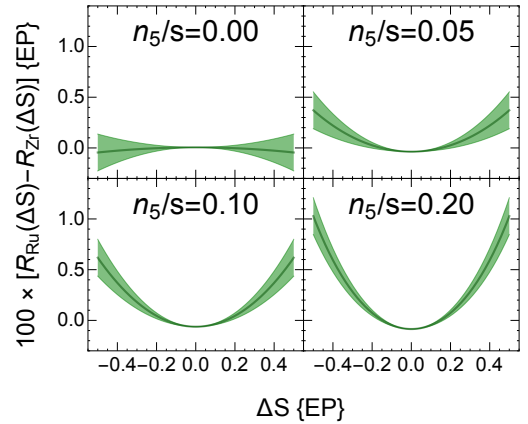


FIG. 6. (color online) Predictions from EBE-AVFD simulations for the R-correlator distributions for $n_5/s = 0\%, 5\%, 10\%$ and 20% respectively (see text for details).

IV. CONCLUSION

In summary, this paper has performed a systematic and quantitative study for the search of Chiral Magnetic Effect in quark-gluon plasma through the isobaric collision experiment at RHIC. To do that, we've developed the necessary and state-of-the-art theoretical tool for describing CME phenomenon in these collisions: the event-by-event anomalous-viscous fluid dynamics (EBE-AVFD) framework. We've also proposed and validated via simulations the best strategy to make isobar subtraction and achieve the best background removal. Based on that, we've made quantitative predictions for a series of charge-dependent azimuthal correlation observables as CME signatures in the collisions of isobars. Such predictions are readily testable and shall soon be verified by anticipated experimental measurements that may likely become available in the next year or so.

Given the predicted signal strength and the present expectation of the achievable measurement precision, we conclude optimistically about the likelihood for a successful extraction of CME signatures in the collisions of isobars. If confirmed indeed, such a detection would not only be the first observation of CME in a chiral material with intrinsically relativistic chiral fermions, but also provide the tantalizing evidence of QCD chiral symmetry restoration in the quark-gluon plasma as well as the unique manifestation of the elusive QCD gluon topological fluctuations.

Acknowledgements.— This work is supported in part by the NSFC Grants No. 11735007 and No. 11875178,

by the NSF Grant No. PHY-1913729 and by the U.S. Department of Energy, Office of Science, Office of Nuclear Physics, within the framework of the Beam Energy Scan Theory (BEST) Topical Collaboration. SS is grateful to the Natural Sciences and Engineering Research Council of Canada for support. The computation of this re-

search was performed on IU's Big Red II cluster, that is supported in part by Lilly Endowment, Inc., through its support for the Indiana University Pervasive Technology Institute, and in part by the Indiana METACyt Initiative. The Indiana METACyt Initiative at IU was also supported in part by Lilly Endowment, Inc.

-
- [1] N. P. Armitage, E. J. Mele and A. Vishwanath, *Rev. Mod. Phys.* **90**, no. 1, 015001 (2018) doi:10.1103/RevModPhys.90.015001 [arXiv:1705.01111 [cond-mat.str-el]].
 - [2] B. Yan and C. Felser, *Ann. Rev. Condensed Matter Phys.* **8**, 337 (2017). doi:10.1146/annurev-conmatphys-031016-025458
 - [3] M. Zahid Hasan, S. Y. Xu, I. Belopolski and S. M. Huang, *Ann. Rev. Condensed Matter Phys.* **8**, 289 (2017) doi:10.1146/annurev-conmatphys-031016-025225 [arXiv:1702.07310 [cond-mat.mtrl-sci]].
 - [4] A. A. Burkov, *Ann. Rev. Condensed Matter Phys.* **9**, 359 (2018) doi:10.1146/annurev-conmatphys-031117-054129 [arXiv:1704.06660 [cond-mat.mes-hall]].
 - [5] D. E. Kharzeev, J. Liao, S. A. Voloshin and G. Wang, *Prog. Part. Nucl. Phys.* **88**, 1 (2016) doi:10.1016/j.ppnp.2016.01.001
 - [6] V. A. Miransky and I. A. Shovkovy, *Phys. Rept.* **576**, 1 (2015) doi:10.1016/j.physrep.2015.02.003 [arXiv:1503.00732 [hep-ph]].
 - [7] K. Fukushima, arXiv:1812.08886 [hep-ph].
 - [8] J. Liao, *Pramana* **84**, no. 5, 901 (2015).
 - [9] K. Hattori and X. G. Huang, *Nucl. Sci. Tech.* **28**, no. 2, 26 (2017) doi:10.1007/s41365-016-0178-3 [arXiv:1609.00747 [nucl-th]].
 - [10] A. Bzdak, S. Esumi, V. Koch, J. Liao, M. Stephanov and N. Xu, arXiv:1906.00936 [nucl-th].
 - [11] D. T. Son and B. Z. Spivak, *Phys. Rev. B* **88**, 104412 (2013) doi:10.1103/PhysRevB.88.104412.
 - [12] Q. Li *et al.*, *Nature Phys.* **12**, 550 (2016) doi:10.1038/nphys3648.
 - [13] Huang, X., Zhao, L., Long, Y., et al. 2015, *Physical Review X*, 5, 031023.
 - [14] Arnold, F., Shekhar, C., Wu, S.-C., et al. 2016, *Nature Communications*, 7, 11615.
 - [15] B. I. Abelev *et al.* (STAR Collaboration), *Phys. Rev. Lett.* **103** (2009) 251601.
 - [16] B. I. Abelev *et al.* [STAR Collaboration], *Phys. Rev. C* **81**, 054908 (2010).
 - [17] L. Adamczyk *et al.* (STAR Collaboration), *Phys. Rev. Lett.* **113** (2014) 052302.
 - [18] B. I. Abelev *et al.* (ALICE Collaboration), *Phys. Rev. Lett.* **110** (2013) 012301.
 - [19] S. Acharya *et al.* [ALICE Collaboration], *Phys. Lett. B* **777**, 151 (2018).
 - [20] V. Khachatryan *et al.* [CMS Collaboration], *Phys. Rev. Lett.* **118**, no. 12, 122301 (2017).
 - [21] A. M. Sirunyan *et al.* [CMS Collaboration], *Phys. Rev. C* **97**, no. 4, 044912 (2018) doi:10.1103/PhysRevC.97.044912 [arXiv:1708.01602 [nucl-ex]].
 - [22] D. E. Kharzeev, L. D. McLerran and H. J. Warringa, *Nucl. Phys. A* **803**, 227 (2008).
 - [23] K. Fukushima, D. E. Kharzeev and H. J. Warringa, *Phys. Rev. D* **78**, 074033 (2008).
 - [24] B. I. Abelev *et al.* (STAR Collaboration), *Phys. Rev. Lett.* **103** (2009) 251601.
 - [25] L. Adamczyk *et al.* (STAR Collaboration), *Phys. Rev. Lett.* **113** (2014) 052302.
 - [26] A. Bzdak, V. Koch and J. Liao, *Lect. Notes Phys.* **871**, 503 (2013)
 - [27] J. Zhao and F. Wang, *Prog. Part. Nucl. Phys.* **107**, 200 (2019) doi:10.1016/j.ppnp.2019.05.001 [arXiv:1906.11413 [nucl-ex]].
 - [28] V. Koch, et al, *Chin. Phys. C* **41**, no. 7, 072001 (2017).
 - [29] D. E. Kharzeev and J. Liao, *Nucl. Phys. News* **29**, no. 1, 26 (2019). doi:10.1080/10619127.2018.1495479
 - [30] J. Błoczyński, X. G. Huang, X. Zhang and J. Liao, *Phys. Lett. B* **718**, 1529 (2013); *Nucl. Phys. A* **939**, 85 (2015).
 - [31] C. Shen, Z. Qiu, H. Song, J. Bernhard, S. Bass and U. Heinz, *Comput. Phys. Commun.* **199**, 61 (2016).
 - [32] C. Gale, S. Jeon and B. Schenke, *Int. J. Mod. Phys. A* **28**, 1340011 (2013) doi:10.1142/S0217751X13400113 [arXiv:1301.5893 [nucl-th]].
 - [33] D. T. Son and P. Surowka, *Phys. Rev. Lett.* **103**, 191601 (2009).
 - [34] S. Shi, Y. Jiang, E. Lilleskov and J. Liao, *Annals Phys.* **394**, 50 (2018) doi:10.1016/j.aop.2018.04.026
 - [35] Y. Jiang, S. Shi, Y. Yin and J. Liao, *Chin. Phys. C* **42**, no. 1, 011001 (2018) doi:10.1088/1674-1137/42/1/011001
 - [36] W. T. Deng, X. G. Huang, G. L. Ma and G. Wang, *Phys. Rev. C* **94**, 041901 (2016); *Phys. Rev. C* **97**, no. 4, 044901 (2018).
 - [37] Y. Sun and C. M. Ko, *Phys. Rev. C* **98**, no. 1, 014911 (2018); *Phys. Rev. C* **95**, no. 3, 034909 (2017). Y. Sun, C. M. Ko and F. Li, *Phys. Rev. C* **94**, no. 4, 045204 (2016).
 - [38] X. L. Zhao, G. L. Ma and Y. G. Ma, *Phys. Rev. C* **99**, no. 3, 034903 (2019). L. Huang, C. W. Ma and G. L. Ma, *Phys. Rev. C* **97**, no. 3, 034909 (2018). Q. Y. Shou, G. L. Ma and Y. G. Ma, *Phys. Rev. C* **90**, no. 4, 047901 (2014).
 - [39] S. Borsanyi, Z. Fodor, S. D. Katz, S. Krieg, C. Ratti and K. Szabo, *JHEP* **1201**, 138 (2012) doi:10.1007/JHEP01(2012)138 [arXiv:1112.4416 [hep-lat]].
 - [40] L. McLerran and V. Skokov, *Nucl. Phys. A* **929**, 184 (2014).
 - [41] U. Gursoy, D. Kharzeev and K. Rajagopal, *Phys. Rev. C* **89**, no. 5, 054905 (2014).
 - [42] K. Tuchin, *Phys. Rev. C* **93**, no. 1, 014905 (2016).
 - [43] G. Inghirami, L. Del Zanna, A. Beraudo, M. H. Moghaddam, F. Becattini and M. Bleicher, *Eur. Phys. J. C* **76**, no. 12, 659 (2016) doi:10.1140/epjc/s10052-016-4516-8 [arXiv:1609.03042 [hep-ph]].
 - [44] U. Gursoy, D. Kharzeev, E. Marcus, K. Rajagopal

- and C. Shen, Phys. Rev. C **98**, no. 5, 055201 (2018) doi:10.1103/PhysRevC.98.055201 [arXiv:1806.05288 [hep-ph]].
- [45] V. Roy, S. Pu, L. Rezzolla and D. H. Rischke, Phys. Rev. C **96**, no. 5, 054909 (2017).
 - [46] S. Pu, V. Roy, L. Rezzolla and D. H. Rischke, Phys. Rev. D **93**, no. 7, 074022 (2016).
 - [47] B. Miller and A. Schfer, Phys. Rev. D **98**, no. 7, 071902 (2018)
 - [48] Y. Guo, S. Shi, S. Feng and J. Liao, doi:10.1016/j.physletb.2019.134929 arXiv:1905.12613 [nucl-th].
 - [49] X. Guo, J. Liao and E. Wang, arXiv:1904.04704 [hep-ph].
 - [50] H. J. Xu, X. Wang, H. Li, J. Zhao, Z. W. Lin, C. Shen and F. Wang, Phys. Rev. Lett. **121**, no. 2, 022301 (2018).
 - [51] S. Shi, H. Zhang, D. Hou and J. Liao, Nucl. Phys. A **982**, 539 (2019).
 - [52] S. A. Voloshin, Phys. Rev. C **70**, 057901 (2004)
 - [53] A. Bzdak, V. Koch and J. Liao, Phys. Rev. C **81**, 031901 (2010) doi:10.1103/PhysRevC.81.031901
 - [54] F. Wang, Phys. Rev. C **81**, 064902 (2010)
 - [55] S. Schlichting and S. Pratt, Phys. Rev. C **83**, 014913 (2011).
 - [56] J. Błoczynski, X. G. Huang, X. Zhang and J. Liao, Nucl. Phys. A **939**, 85 (2015) doi:10.1016/j.nuclphysa.2015.03.012 [arXiv:1311.5451 [nucl-th]].
 - [57] F. Wen, J. Bryon, L. Wen and G. Wang, Chin. Phys. C **42**, no. 1, 014001 (2018) doi:10.1088/1674-1137/42/1/014001
 - [58] H. j. Xu, J. Zhao, X. Wang, H. Li, Z. W. Lin, C. Shen and F. Wang, Chin. Phys. C **42**, no. 8, 084103 (2018)
 - [59] J. Zhao, H. Li and F. Wang, Eur. Phys. J. C **79**, no. 2, 168 (2019)
 - [60] L. Huang, M. W. Nie and G. L. Ma, arXiv:1906.11631 [nucl-th].
 - [61] S. Choudhury, G. Wang, W. He, Y. Hu and H. Z. Huang, arXiv:1909.04083 [hep-ph].
 - [62] N. Magdy, S. Shi, J. Liao, N. Ajitanand and R. A. Lacey, Phys. Rev. C **97**, no. 6, 061901 (2018) doi:10.1103/PhysRevC.97.061901
 - [63] N. Magdy, S. Shi, J. Liao, P. Liu and R. A. Lacey, arXiv:1803.02416 [nucl-ex].